Molecular Therapy
Oncolytics
Original Article

AMERICAN SOCIETY of GENE & CELL THERAPY

IRS2 Amplification as a Predictive Biomarker in Response to Ceritinib in Small Cell Lung Cancer

Mi-Sook Lee,[1,2,3] Kyungsoo Jung,[1,2,3] Ji-Young Song,[1] Min-Jung Sung,[1] Sung-Bin Ahn,[1,2] Boram Lee,[2] Doo-Yi Oh,[1,2,4] and Yoon-La Choi[1,2]

[1]Department of Pathology and Translational Genomics, Samsung Medical Center, Sungkyunkwan University School of Medicine, Seoul 06351, Korea; [2]Department of Health Sciences and Technology, Samsung Advanced Institute for Health Sciences & Technology, Sungkyunkwan University, Seoul 06351, Korea

Small cell lung cancer (SCLC) is a fast-growing and malignant cancer that responds well to chemotherapy; however, the survival rate is less than 15% after 2 years of diagnosis. Therefore, novel therapeutic agents for treating SCLC patients need to be evaluated. This study aims to identify the therapeutic targets based on the comprehensive genomic profiling of SCLC patients. Among the molecular-profiled SCLC samples obtained using targeted sequencing, the array-based comparative genomic hybridization (array CGH) identified focal *insulin receptor substrate 2* (*IRS2*) amplification in the SCLC patients. *IRS2* amplification was confirmed in 5% of 73 SCLC patients. To determine whether *IRS2* amplification could act as a therapeutic target, we generated a patient-derived xenograft (PDX) model and subsequently screened 43 targeted agents using the PDX-derived cells (PDCs). Ceritinib significantly inhibited the cell growth and impaired the tumor sphere formation in IRS2-expressing PDCs. Its effects were confirmed in various *in vitro* assays and were further validated in the mouse xenograft models. In this study, we present that *IRS2* amplification and/or expression serve as preclinical implications for a novel therapeutic target in SCLC progression. Furthermore, we suggest that insulin-like growth factor-1 (IGF-1) receptor inhibitor-based therapy could be used for treating SCLC with *IRS2* amplification.

INTRODUCTION

Small cell lung cancer (SCLC) mainly arises in heavy smokers and has been characterized with rapid growth and early spread.[1–3] SCLC accounts for approximately 15% of lung cancer, and chemotherapy is currently the standard treatment; however, a recurrence occurs in most cases, and with eventually a 7%, 5-year survival.[2–4] To date, there have been increased efforts to understand the biological characteristics of SCLC and to excavate therapeutic targets based on the molecular signatures.[2,5] Previous studies applying sequencing in SCLC tumor specimens have reported that SCLC genomes exhibit considerable mutation rates and genomic instability, and in the majority of the tumors, they present universal inactivation of tumor protein p53 (*TP53*) (75%–90% of cases), the retinoblastoma gene (retinoblastoma 1 [*RB1*], ~65%), and amplification of the *MYC* family genes.[6–9] However, no drug has revealed therapeutic efficacy and survival benefit in patients with the corresponding mutations.[1] Accordingly, the targeted treatment in SCLC offers to improve the efficacy of standard chemotherapy and chemoradiotherapy by concurrent administration or to use it after failure of the standard treatment.[5]

Insulin receptor substrate 1 (IRS1) and IRS2 proteins are the most prominent signal transmitters from either the insulin-like growth factor-1 receptor (IGF-1R) or the insulin receptor, and this pathway activates the phosphatidylinositol 3-kinase (PI3K)-AKT pathway, thus leading to cell proliferation and inhibition of programmed cell death.[10,11] Hence, molecules within the IGF-1 signaling pathway are the potential therapeutic targets in cancer. Although, in the preclinical *in vitro* study, blockade of the IGF-1R inhibits the growth and malignancy of tumor into a valid targeted therapy, a single treatment with the IGF-1R inhibitor failed to demonstrate the clinical benefits for the overall survival (OS) of patients in several clinical trials.[12] Targeted therapies for the IGF-1R pathway have a low clinical response rate in the unselected patients; however, IGF-1R still remains a rational target for a certain tumor.[13] Therefore, the strategies combining a therapeutic inhibitor in the IGF-1R pathway with chemotherapy could be useful for treating selected subtypes with a predictive biomarker.

Received 26 July 2019; accepted 23 December 2019;
https://doi.org/10.1016/j.omto.2019.12.009.

[3]These authors contributed equally to this work.

[4]Present address: Department of Otorhinolaryngology-Head and Neck Surgery, Seoul National University Bundang Hospital, Seoul National University College of Medicine, Seongnam 13620, Korea.

Correspondence: Doo-Yi Oh, PhD, Department of Otorhinolaryngology-Head and Neck Surgery, Seoul National University Bundang Hospital, Seoul National University College of Medicine, Seongnam 13620, Korea.
E-mail: dooyi9@gmail.com
Correspondence: Yoon-La Choi, MD, PhD, Department of Pathology and Translational Genomics, Samsung Medical Center, Sungkyunkwan University School of Medicine, Irwon-ro 81, Gangnam-gu, Seoul 06351, Korea.
E-mail: ylachoi@skku.edu

Most insulin/IGF1 signaling in the lungs converges into intracellular IRS1/2 adaptor proteins before diverging to the downstream signals, including PI3K, AKT, and mTOR, which are regulated by complex signaling networks.[14] IRS1/2 mediates mitogenic and antiapoptotic signaling from IGF-1R and insulin receptor (IR) and other oncoproteins. IRS1 plays a crucial role in cancer cell proliferation, its expression is increased in various human malignancies, and its upregulation mediates resistance to the anticancer drugs. IRS2 is associated with cancer cell motility and metastasis.[15] Concomitant ablation of *Irs1/Irs2* in the genetically engineered mouse lung model with conditional *Kras* activation and *p53* loss strongly suppresses the tumor initiation and extends tumor latency, due to decreased amino acid uptake resulting from suppressed growth factor signaling in the tumor cells.[14] These findings provide evidence that *IRS1/2* is required for *KRAS* mutant lung cancer formation, and targeting of the IGF-1R signaling pathway could be a valuable therapeutic strategy in treating *KRAS* mutant non-SCLC (NSCLC).[14] Huang et al.[16] reported that *IRS2* copy number gain harboring the *KRAS* or *BRAF* mutation could potentially be considered as a predictive biomarker in response to the IGF-1R/IR inhibitor in colorectal cancer harboring the *KRAS* or *BRAF* mutation.

Here, we generated patient-derived xenografts (PDXs) from SCLC obtained via brain metastasis and analyzed genomic profiling. Thus, we identified the *IRS2* amplification and evaluated its potency as a therapeutic target by drug screening and proved that ceritinib decreased the *in vitro* cell proliferation and *in vivo* tumor growth in IRS2-expressing cells. These preclinical data imply that IRS2 amplification or expression (or both) could be a therapeutic biomarker and that ceritinib could prove to be a therapeutic agent for SCLC patients.

RESULTS

Identification of Aberrant IRS2 Expressions in SCLC Patient

A 61-year-old male patient subjected to chest computed tomgraphy (CT) presented a 5.8-cm-sized mass in the left lower lobe of the lung with multiple enlarged ipsilateral mediastinal and hilar lymph nodes during diagnosis. The patient was diagnosed with an SCLC with limited stage and received etoposide and paclitaxel-based chemotherapy with concurrent radiation therapy. The patient achieved complete remission on follow-up imaging studies after completing the scheduled treatment. After 2 years, the malignant tumor cells morphologically consistent with the SCLC were identified by the pericardial fluid. Palliative chemotherapy based on irinotecan and carboplatin was administered, and a second complete remission was recorded after the therapy. After another 2 years, the brain magnetic resonance imaging (MRI) revealed a huge metastatic lesion on the right parietal lobe (Figure 1A). The tumor was removed, followed by whole body radiation therapy. To identify an origin for the metastatic tumor, it was stained with lung cancer markers, including thyroid transcription factor 1 (TTF1), p63, and CD56, and presented strong positive staining for TTF1 and CD56, which are used as markers in diagnosing SCLC (Figure S1A). To investigate the target for personalized cancer therapy from this case (694T), a PDX model was established with a metastatic small-cell carcinoma sample obtained from brain metastasis, and the PDX-derived tumor cells were subjected to *in vitro* assays.

To validate the genetic similarity of 694T parental tumors, PDX tumors, and PDX-derived cells (PDCs), comparative genomic hybridization (CGH) analysis was performed (Figure 1B). The results revealed that, by copy number analysis, the focal amplification of known oncogene loci, *MYCL1*, was carried out, and a novel chromosomal region was amplified on the chromosomes 1p34.2 and 13q33 (Figure 1B; Figure S1). *MYC* family genes were frequently detected in SCLC[17] and amplified in the 1p34.2 region of 694T parental tumors, PDX tumors, and PDCs (Figure S1B). A novel chromosomal amplification was illustrated on 13q33 loci in the 694T-PDX and parental SCLC tumor (Figure 1C). Within this 13q33 amplicon, myosin XVI (*MYO16*), collagen type IV alpha 1 chain (*COL4A1*), and *IRS2* were localized. Amplification of *MYO16* or *COL4A1* in the initiation and progression of tumors remains unknown. *IRS2* triggers the driver oncogene on 13q34 in colorectal cancer,[18] and we hypothesized that *IRS2* copy number gain among the three genes has an oncogenic role in SCLC progression. The IRS2 was highly expressed in the 694T-PDX and parental tumor (Figure 1D). To further investigate how the tumor signaling pathway was regulated by IRS2 overexpression, we performed microarray experiments with all samples (Figure 2A). The result indicated that highly expressed molecules such as IGFBP-2, AKT1, and mTOR were associated with the IGF-1R signaling pathway, and no significant differences were observed in the expression pattern among the samples. These results were confirmed by western blotting using the PDX of the 694T patient. The tumor expressed the increased phosphorylation of AKT, compared with the 033T sample, which has no IRS2 amplification and/or expression as a negative control (Figure 1E). With these data taken together, we concluded that *IRS2* copy number amplification leads to abnormal expression of IRS2 and induces activation of AKT.

Frequency and Clinical Significance with IRS2 Copy Number Alterations in SCLC

In order to assess the population of *IRS2* focal amplifications in SCLC, we conducted immunohistochemistry (IHC) analysis in 73 randomly selected SCLC patients. The IHC test score of 0–3 measures the amount of IRS2 expression in the tumor cells, a score of 0–1 was considered as a negative, and a score of 2 or higher was regarded as a positive sample (Figure 2B). IRS2 was positively expressed in 32.9% (n = 24) in 73 stained samples, and *IRS2* amplifications were determined in the available 77 SCLC samples using qRT-PCR (Figure 2C). Interestingly, the focal amplification with *IRS2* high copy number 10 or higher occurred in four cases (Figure 2C). Our observation was similar to the frequency that was previously reported in SCLC.[6] To investigate the clinical implications of *IRS2* gain/amplification in cancer progression, we analyzed the SCLC dataset that is publicly available via the cBioPortal for Cancer Genomics (http://www.cbioportal.org/msk-impact). *IRS2* amplification was detected in 2.44% (n = 2) of 82 SCLC cases (Figure 2D). The clinical characteristics of the SCLC patients by IRS2 expression are listed in Table 1. In the chi-square analysis, the IRS2 expression in the females was

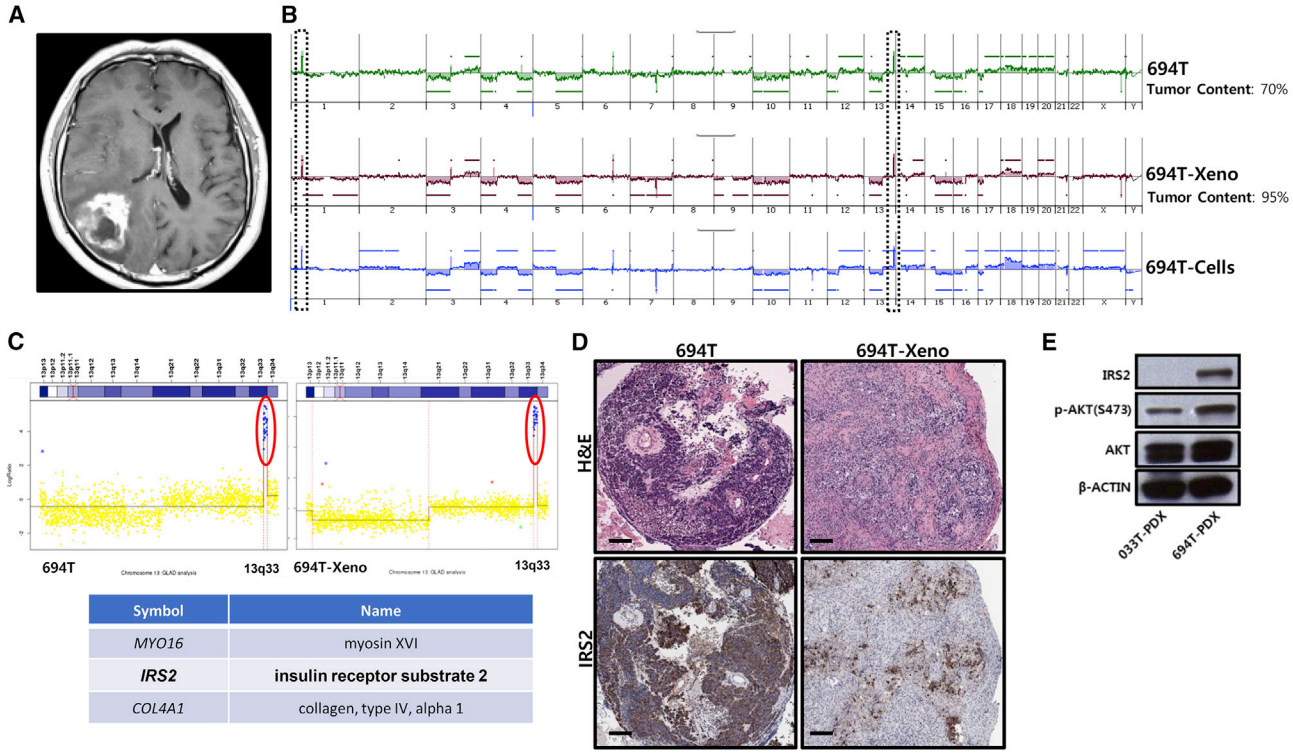

Figure 1. Expression of IRS2 with Copy Number Amplification in SCLC Primary Tumor and PDX Models

(A) Brain MRI revealed a huge metastatic lesion on the right parietal lobe in the 694T patient. (B) Genetic features of the patient-derived tumors were recapitulated by PDX and PDC counterparts, using aCGH. (C) *IRS2* was amplified in the patient-derived tumors and PDX samples. (D) Histological comparison between the patient tumor sample and PDX tumor. The representative areas of each patient tumor sample and the corresponding PDXs were stained with hematoxylin and eosin (H&E) and IRS2 antibodies. IRS2 immunohistochemical staining revealed distinctive expression patterns both in the 694T patient-derived tissue and PDX tumor samples. Magnification, 400×. Scale bars, 100 μm. (E) IRS2, phosphorylated AKT, AKT, and β-actin as a loading control were analyzed using western blot in 649T patient tumor. Patient 033T samples were used as negative controls.

significantly higher ($p = 0.0313$), and significant differences were observed in IRS2 expression in the nonsmoker group, regardless of gender ($p = 0.0374$). No significant difference was observed during survival between the two groups ($p = 0.9264$); however, although few cases provide statistical meaning, four patients with *IRS2* amplification have shown improved progression-free survival (PFS), compared to patients without *IRS2* amplification and/or expression (data not shown).

Ceritinib Inhibits the Cell Proliferation via IRS2-PI3K Axis

To explore the applications of targeted anticancer therapeutics in IRS2-expressing tumor, we performed a preclinical drug screening, and the half maximal inhibitory concentration (IC_{50}) values for target agents were obtained from the PDCs in the *in vitro* sphere culture conditions (Figure 3A; Table S1). According to the previously reported results,[19] the cells are considered as resistant to an agent when the IC_{50} of that agent is greater than 1,000 nmol/L. The proliferation of 694T cells was not affected by the epidermal growth factor receptor (EGFR) inhibitors, such as erlotinib (IC_{50} = 3,118 nmol/L) and gefitinib (IC_{50} = 1,562 nmol/L); however, PDCs with IRS2 amplification, such as LDK378 (ceritinib) (IC_{50} = 0.413) and NVP-AEW541 (IC_{50} = 0.218), responded to the IGF-1R inhibitor treatment (Figure 3A; Table S1). Additionally, AZD2014 (IC_{50} = 282 nmol/L) and dactolisib (IC_{50} = 90 nmol/L), the PI3K/mTOR inhibitors, were effective against 643T PDCs (Table S1). Treatment with ceritinib at 0.5 μM decreases the *in vitro* sphere-forming capacity and proliferation by abolishing the phosphorylation of AKT, a downstream signaling component of IGF-1R in 694T PDCs (Figure 3B). To confirm the effect of ceritinib in IRS2-expressing cancer progression, *IRS2* was transduced into HCC33 and H1299 lung cancer cells that do not express IRS2, followed by treatment with ceritinib at doses of 0.1–5 μM (Figures 3C and 3D). Overexpression of IRS2 increased AKT phosphorylation, and IRS2-expressing cells decreased the proliferation and phosphorylation of AKT when they were treated with ceritinib (Figures 3C and 3D). These results demonstrate that ceritinib decreases the IRS2-overexpressing cell growth via inhibition of AKT activation.

Ceritinib Inhibits the Tumor Growth via IRS2-PI3K Axis

We attempted to confirm the ceritinib effect using cell lines with high-level expression of endogenous IRS2. Based on the Cancer Cell Line Encyclopedia (CCLE) Cell Line Gene Expression Profiles dataset,

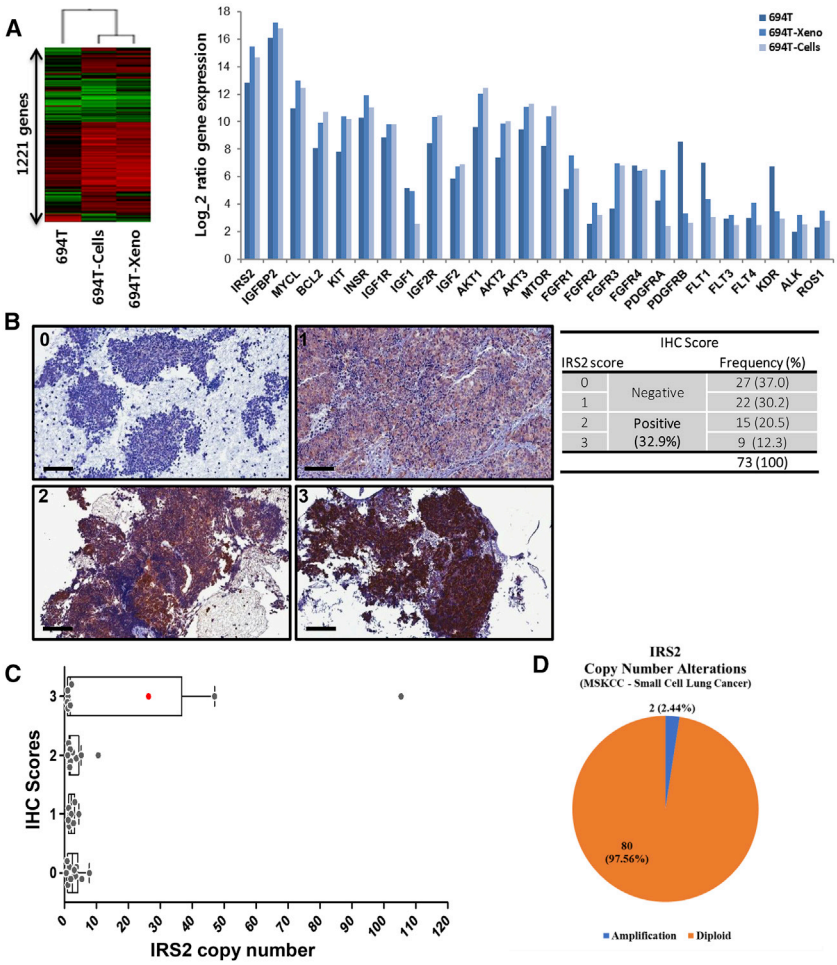

Figure 2. Gene Expression Profiling and Frequency with *IRS2* Amplification in SCLC

(A) The heatmap presents the status of 1,221 gene expressions in the microarray analysis of 694T patient-tumor, PDX, and PDC samples, and the top 20 significantly expressed genes across all samples are illustrated. (B) IRS2 expression in 73 paraffin-embedded SCLC tissues (400×). The samples are stained with IRS2 antibodies and scored according to the levels of expression. A score of 2 or higher was regarded as positive. Scale bars, 100 μm. (C) *IRS2* copy number amplification is analyzed using quantitative PCR (qPCR). A boxplot represents the mean value of the *IRS2* copy number in the group, and the red dot represents the *IRS2* copy number in 694T patient tissue. Experiments were performed in triplicate. (D) *IRS2* amplification was detected in 2.44% (n = 2) of 82 SCLC cases. The analysis of focal amplifications in the SCLC dataset is publicly available through the cBioPortal for Cancer Genomics (n = 82).

we selected an A375P cell line that considerably expresses IRS2 relative to other cell lines (https://portals.broadinstitute.org/ccle/page?gene=IRS2). To investigate the effects of IRS2 depletion on A375P cell growth, the cells were treated with small interfering RNA (siRNA). Downregulation of IRS2 expression by siRNA led to A375P cell growth inhibition and AKT phosphorylation (Figure 4A). To further validate whether treatment with ceritinib affected the A375P cell growth, cells were treated with ceritinib and were analyzed as presented in Figure 4B. Cells treated with ceritinib revealed decreased proliferation and AKT phosphorylation in a dose-dependent manner (Figure 4B). To evaluate the *in vivo* efficacy of ceritinib, A375P cells were subcutaneously injected into the flanks of nude mice on day 1, and the tumor growth was monitored. After 10 days, the tumor-bearing mice were treated with ceritinib (20 or 50 mg/kg) on every other day for 17 days, and the tumor size was measured. As expected, marked tumor regression was observed in the treatment groups, and the mice treated with ceritinib at 50 mg/kg led to more effective tumor regressions (Figure 4C). The tumors were stained with IRS2 and phospho-AKT (Ser473) antibodies to evaluate the expression and activation of these molecules. IRS2 was highly expressed and increased AKT phosphorylation in A375P tumors; however, these tumors, when treated with 50 mg/kg ceritinib, hindered IRS2 expression and decreased AKT phosphorylation, compared with the control group (Figure 4D). These results demonstrate that ceritinib leads to the inhibition of IRS2-overexpressing tumor growth by inactivation of AKT through depletion of IRS2.

DISCUSSION

PDXs are used as a prominent cancer model system, as they are presumed to faithfully represent the genomic features of primary tumors. Here, we established histopathologically and genomically homologous PDX models of metastatic tumor from SCLC and found a patient with aberrant *IRS2* amplifications. In this study, we elucidated that *IRS2* amplification could be a target of response to the IGF-1R pathway inhibitors and demonstrated this via preclinical *in vitro* and *in vivo* assays. Ceritinib, an ALK/IGF-1R dual-inhibitor agent, had inhibitory effects on the proliferation of tumor cells with *IRS2* amplification, and this result was confirmed in the xenograft model. From these findings, we suggest that IRS2 amplification and/or expression could be a predictive biomarker of response to the IGF-1R inhibitor-based therapy in SCLC progression.

The SCLC genome exhibits extremely high mutation rates and harbors inactivated *RB1* and *TP53*.[6] To comprehensively determine the genomic features of the tumor in the 694T patient with brain metastases from SCLC, we conducted CGH arrays and targeted sequencing using the CancerSCAN panel, which includes the whole exomes of 375 cancer-related genes and the intronic regions of 23 genes. Our patient genome presented the somatic mutations of *TP53*, *PDGFRB*, *ARID1A*, *PTCH1*, and *JAK3* genes but not *RB1*, which were well conserved in the multiple passages (Figure S2A); however, these mutations do not occur recurrently in the cosmic database as driver mutations.

Table 1. Clinicopathological Characteristics of 73 SCLC Patients

Characteristic	Positive (n = 26)	Negative (n = 47)	p
Age (in Years)			
Median (and range)	67 (51–87)	68 (33–82)	
Sex, n (and %)			
Male	18 (69.2%)	42 (89.4%)	0.0313
Female	8 (30.8%)	5 (10.6%)	
Stage, n (and %)			
Limited disease	10 (38.5%)	15 (32.0%)	0.6316
Extended disease	14 (53.8%)	27 (57.4%)	
ND	2 (7.7%)	5 (10.6%)	
Smoking History, n (and %)			
Smokers (currently and former)	21 (80.8%)	45 (95.8%)	0.0374
Never smokers	5 (19.2%)	2 (4.2%)	
Chemotherapy, n (and %)			
Etoposide + cisplatin (EP)	10 (38.5%)	22 (46.8%)	
EP + IC (irinotecan + carboplatin)	7 (26.9%)	6 (12.8%)	0.3702
Others	7 (26.9%)	12 (25.5%)	
No chemotherapy	2 (13.9%)	7 (14.9%)	
Radiotherapy, n (and %)			
Yes	8 (30.8%)	17 (36.2%)	0.6415
No	18 (69.2%)	30 (63.8%)	
Recurrence, n (and %)			
No	19 (73.1)	31 (67.4%)	0.5306
Yes	7 (26.1%)	16 (34.0%)	
Local	2/7 (28.6%)	1/16 (6.2%)	
Distance	5/7 (71.4%)	15/16 (93.8%)	
OS, n (and %)			
Death	11 (42.3%)	21 (44.7%)	0.9264
Alive	13 (50.0%)	26 (55.3%)	
ND*	2 (7.7%)		

ND, no data; OS, overall survival.

Additionally, within the chromosomal regions 1p34.2 and 13q34, *MYCL1* and *IRS2* revealed significant focal co-amplification. To date, amplification of *MYCL* in SCLC is one of the common alterations including *TP53* and *RB* mutations, and recently reported studies have shown that *MYCL* is not a major driver oncogene but has a cooperative role in accelerating SCLC tumor growth.[20–22] IRS2 enhances glucose metabolism and promotes migration, invasion, and metastasis in various type of tumors.[16,18,23–26] However, it is not well known for clinical outcomes of the IRS2 expression in lung cancer progression, so we focused on *IRS2* amplification and conducted various experiments to validate whether *IRS2* amplification and/or expression is a therapeutic biomarker in metastatic SCLC.

IRS2 is known as a candidate driver oncogene on 13q34 in colorectal cancer.[18] *IRS2* copy number gain and/or expression was observed to be sensitive to the IGF-1R/IR inhibitor and could be used as a predictive biomarker in response to the IGF-1R/IR inhibitor, such as *KRAS* and *BRAF* mutational status in colorectal cancer cell lines.[16] Recently, another study also has suggested that *IRS1* and *IRS2* are required for *KRAS* mutant lung cancer formation, and they may be therapeutic targets in patients with *KRAS* mutant lung cancer.[14] Therefore, despite the presence of *MYCL1* amplification, we elucidated that *IRS2* would be a reliable biomarker for treatment in this patient via *in vitro* assays and an *in vivo* xenograft model. To further investigate for clinical outcomes of IRS2 amplification and/or expression in lung cancer, we demonstrated the frequency of IRS2 amplification and/or expression in 73 SCLC patients and determined the clinicopathological features of the patients with or without IRS2 expression. As presented in Table 1, IRS2 expression is statistically significantly higher in females and nonsmokers. Interestingly, our 694T patient has a good prognosis after treatment, unlike other SCLC patients, despite having a smoking history. These findings have led us to investigate the PFS of SCLC patients with IRS2 amplification and/or expression; however, we were unable to analyze the clinical significance including PFS or OS, due to the lack of clinical information and limitations of the sample size. In our cohort, female patients with IRS2-overexpressing SCLC showed a tendency toward a longer PFS, but no statistical significance was observed (data not shown). Collectively, we suggest that *IRS2* amplification has been detected at a low frequency in SCLC but may be a subtype biomarker to predict the treatment benefit.

To assess the possibility for targeted therapy, we carried out *in vitro* experiments using PDCs and cancer cell lines with or without IRS2 expression (Figure 3). We demonstrated that the cells overexpressing IRS2 increased the growth via PI3K/AKT pathways and that this growth was inhibited by ceritinib treatment. Ceritinib (LDK378, Novartis Pharmaceuticals) binds to the tyrosine kinase receptors and inhibits ALK, IGF-1R, insulin receptor (InsR), and ROS1 on the cell surface. By binding to these receptors, ceritinib suppresses ALK phosphorylation as well as the downstream PI3K/AKT, MEK/ERK, and mTOR signaling pathways and blocked the cell proliferation in NSCLCs.[27] Hence, the genomic profile in a 694T patient was identified by array-based comparative genomic hybridization (aCGH), and no amplification was observed in the *ALK* gene (Figure S2B). This supports the statement that IRS2 amplification and/or overexpression could be a potential target in treatment of ceritinib. This was confirmed in that the cell growth with endogenously high expression of IRS2 was inhibited with treatment of ceritinib or IRS2 repression by siRNAs, and tumor volume finally decreased in IRS2-expressing xenografts with ceritinib treatment (Figure 4). As shown in Figure 4D, AKT have shown moderate expression pattern in IRS2-expressing xenograft tumors and the expression has been weak by ceritinib treatment. Therefore, these results suggest that ceritinib could represent a suitable treatment option in patients with IRS2 amplification and/or expression.

Although IRS2 amplification and/or expression is a feature of some but not all human SCLC, our finding demonstrates that patients with IRS2 amplification and/or expression could be a selected group

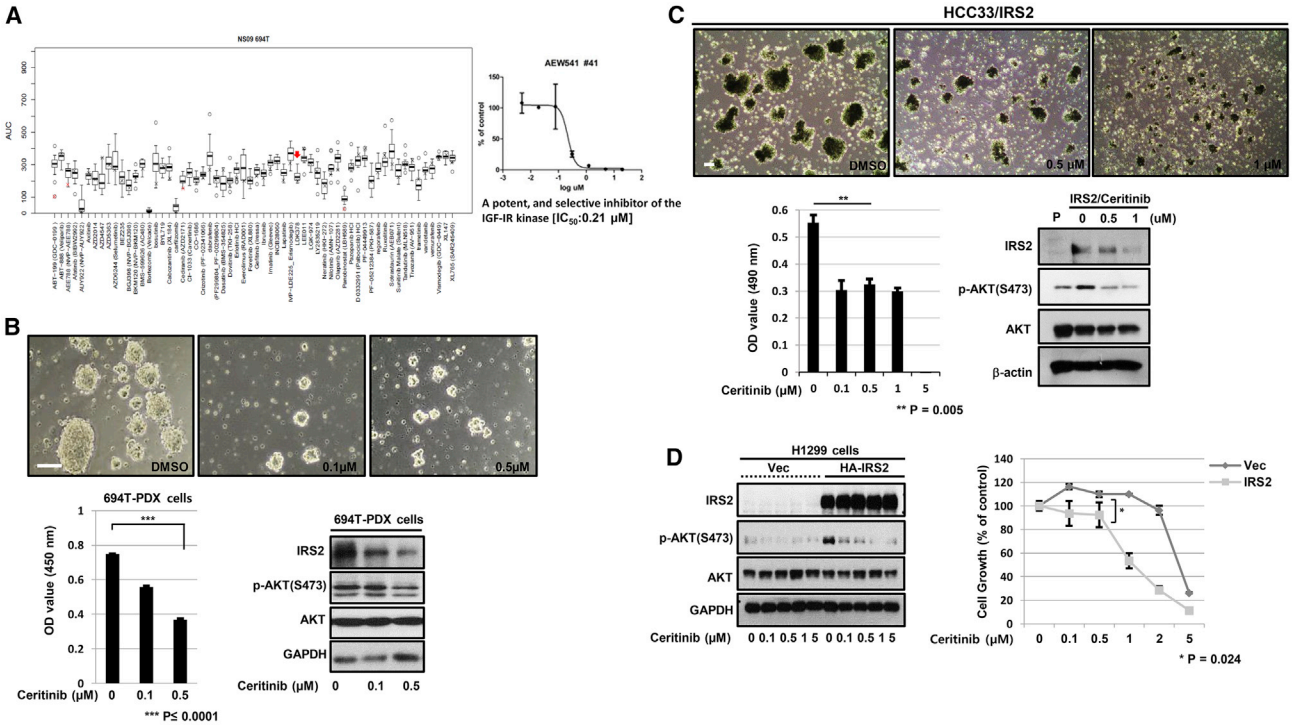

Figure 3. Growth Inhibition with Ceritinib in IRS2-Expressing Cells

(A) Proliferation of 694T cells was found to be decreased by IGF1 inhibitors LDK378 (red arrow) and AEW541 using an *in vitro* drug sensitivity assay. 694T PDCs were cultured from the established 694T patient xenograft tumors in serum-free sphere culture conditions and were plated into 386-well cell-culture plates and treated with drug candidates, with improved therapeutic and safety profiles in lung cancer, for 6 days. Drug efficacy was evaluated as a mean of area under concentration-response curve (AUC), and x represents drugs with a *Z* score less than −1.5. Detailed responses of PDCs to drugs are shown in Table S1. NVP-AEW541 is an IGF-IR inhibitor with a median IC_{50} of 0.21 μM. (B) Treatment with ceritinib inhibited cell proliferation through AKT inactivation and significantly impaired sphere formation. 694T cells were cultured from day 5 onward with or without ceritinib. On day 5, phase-contrast microscopic images were visualized, and optical density assays to determine cell proliferation were performed (bottom left). Representative immunoblots of the indicated proteins in lysates of 694T cells treated with ceritinib were obtained (bottom right). 694T cells treated with ceritinib showed a reduction in phosphorylated AKT and IRS2 expression. Experiments were performed in triplicate. Magnification, 200×. Scale bar, 100 μm. Treatment with ceritinib impaired cell proliferation in IRS2-expressing (C) HCC33 and (D) H1299 cell lines. Cells expressing IRS2-expressing vector. Cells expressing IRS2 were treated with different concentrations of ceritinib in the range of 0.1–5000 nM for 72 h, images were obtained, and the absorbance was measured at 490 nm. Means ± SD from three independent experiments. IRS2 and phosphorylated AKT were analyzed using western blot in the cells with or without IRS2 expression. Magnification, 200×. Scale bar, 100 μm. (D) Cell growth was analyzed as a percentage to the control. Experiments were performed in triplicate. Means ± SD from three independent experiments.

for a targeted therapy and unique vulnerability to IGF-1R pathway inhibitors such as ceritinib, suggesting a repositioning of ceritinib as a therapeutic approach based on the genomic profile in SCLC.

MATERIALS AND METHODS

Patient Tissue Samples

This study and all the experimental procedures were approved by the Samsung Medical Center (Seoul, Korea) Institutional Review Board, and written informed consents were obtained from all participants (no. 2010-04-004). Tumors were classified as SCLCs, based on the World Health Organization (WHO) criteria. Patients were categorized as nonsmokers (<100 cigarettes in their lifetime) or chain smokers (≥100 cigarettes in their lifetime) based on their smoking status. SCLC histological subtypes and stages were classified according to WHO criteria[28] and the American Joint Committee on Cancer staging system,[29] respectively. Surgical specimens were divided into three parts, for implantation into immunodeficient mice, DNA/RNA extraction, and pathologic assessment, within 6 h after surgery. Nonmalignant normal lung tissue samples were collected from the far margins of the lung resections, which were grossly and microscopically negative for the tumor tissue. Lung tissue samples were minced with scalpels into 1-mm pieces and were then enzymatically disaggregated to create single-cell suspensions by incubating them with 1 mg/mL collagenase P (Roche Genentech, San Francisco, CA, USA) and 0.1 mg/mL DNase I (Applied Biosystems, Foster City, CA, USA) in RPMI 1640 medium with 10% fetal calf serum (FCS) for 16 h, with constant stirring. Each well of a 6-well culture plate (Corning, Corning, NY, USA) was inoculated with 100×10^3 viable cells in 4 mL RPMI 1640 medium with 10% FCS.

Primary *In Vitro* Short-Term Culture

Xenograft tumor specimens were dissociated into single cells according to a previously published protocol.[16] Dissociated cells were cultured in Neurobasal medium-A, supplemented with N2 (×1/2; Life

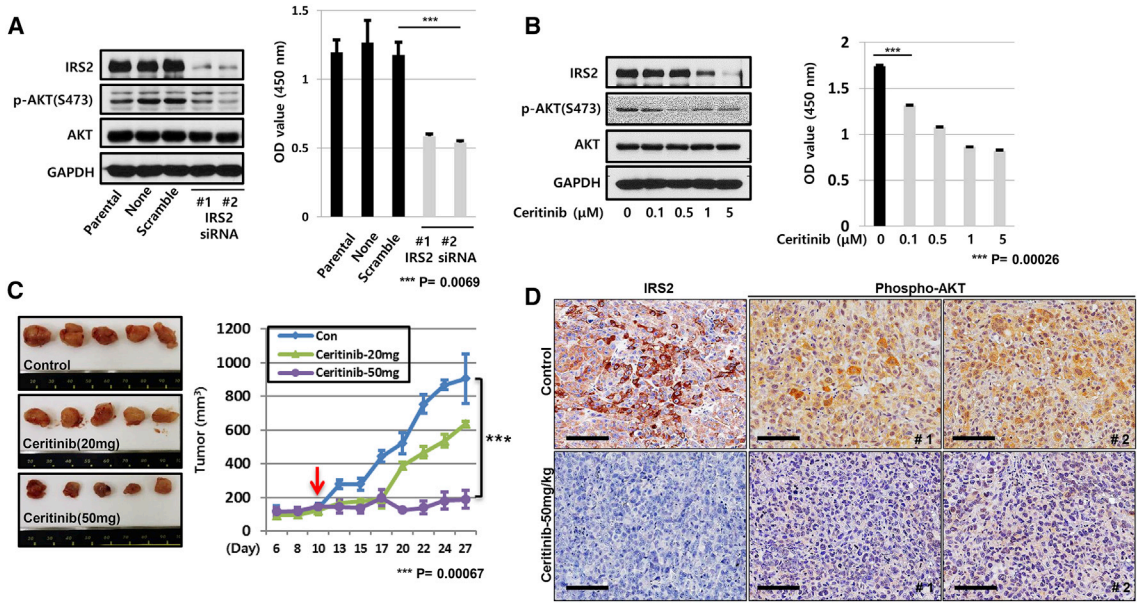

Figure 4. Tumor Growth Inhibition with Ceritinib in Xenograft Model

(A) Treatment of A375P cells with IRS2 siRNA (#1 and #2) results in reduced activation of phospho-AKT (Ser473). GAPDH levels serve as control. OD, optical density. (B) Treatment with ceritinib impaired the cell proliferation in A375P cells. Cells were treated with or without ceritinib in the indicated doses for 72 h, and the expression levels of IRS2, phospho-AKT, AKT, and GAPDH were determined by western blotting. Cell proliferation was quantitatively evaluated by WST assay. Means ± SD from three independent experiments. (C) A total of 15 nude mice were subcutaneously inoculated with A375P cells (≈5×10^6) in the right flank. After 10 days, the tumor-bearing mice were treated with ceritinib (20 or 50 mg/kg) on every other day for 17 days; changes in tumor volume over time following the treatment are indicated (red arrow). Data points represent the mean ± SD of tumor volumes from each group (n = 5). (D) Representative images of IRS2 and phosphorylated AKT (Ser473) staining in mice xenografts from each group. Magnification, 400×. Scale bars, 100 μm.

Technologies, Carlsbad, CA, USA), B27 (×1/2; GIBCO), basic fibroblast growth factor (bFGF; 25 ng/mL; R&D Systems, Minneapolis, MN, USA), epidermal growth factor (EGF) (25 ng/mL; R&D Systems, Minneapolis, MN, USA), neuregulin 1 (NRG; 10 ng/mL; R&D Systems, Minneapolis, MN, USA), and IGF1 (100 ng/mL; R&D Systems, Minneapolis, MN, USA). Growth factors were supplemented every 3 days. When spheres appeared in the suspension culture, they were dissociated using StemPro Accutase (Life Technologies, Carlsbad, CA, USA) and reseeded in the suspension culture medium. Cells were grown in complete medium and were treated with inhibitors 1 day after seeding. Five days later, the surviving cells were quantified by WST-1 staining (Roche Genentech, San Francisco, CA, USA).

Cell Lines

The H1299, A375P, and NCI-HCC33 cell lines were obtained from the Korean Cell Line Bank (KCLB; Seoul, Korea), and maintained in RPMI 1640 medium supplemented with 10% fetal bovine serum (Thermo Fisher Scientific, Grand Island, NY, USA) at 37°C in 5% CO_2. All of the cell lines used were authenticated by short tandem repeat (STR) profiling before a new series of experiments began and were preserved in the culture for no more than 3 months.

Histological Examination and IHC

Hematoxylin and eosin (H&E) staining was performed on all paraffin blocks with the tissue samples obtained from both patients and PDXs. The anti-IRS2 (Abcam, Cambridge, MA, USA, EPR904(2)) and anti-phospho-AKT (Cell Signaling Technology, 3787) antibodies were used for IRS2 and p-AKT immunohistochemical staining. The sections (3 μm) were deparaffinized and rehydrated, and antigen retrieval was performed in a citrate buffer (pH 6.1) at 95°C for 40 min. Diaminobenzidine was used as the chromogen. The sections were counterstained with hematoxylin. The BenchMark XT IHC/ISH staining instrument (Ventana Medical Systems, Tucson, AZ, USA) was utilized. IRS2-expressing cancer tissues were used as positive controls.

aCGH

The aCGH detected genetic variations, including deletions and duplications, using the Agilent Human Whole Genome CGH 8 × 60 K microarray (Agilent Technologies, Santa Clara, CA, USA). Test and reference DNA samples were labeled by random priming with either Cyanine 3 labeled analog of deoxyuridine triphosphate (dUTP) or Cy5-dUTP using the Agilent Genomic DNA Labeling Kit PLUS (Agilent Technologies). All slides were scanned on an Agilent DNA microarray scanner. Data were obtained using Agilent Feature Extraction Software 9 (Agilent Technologies), which was used to analyze the ADM-2 statistical algorithms with 6.0 sensitivity thresholds, as described previously.[19]

Genetic Alteration Analysis Using the Cancer Panel

The Cancer Panel is a targeted next-generation sequencing assay that was developed, validated, and provided by the Samsung Genome

Institute (Samsung Medical Center, Seoul, Korea). It includes all exons from 381 cancer-related genes and 31 introns from five genes recurrently rearranged in cancer. Using the Illumina HiSeq 2500 (San Diego, CA, USA), the captured libraries underwent paired-end high-depth sequencing (target > 800 × coverage). Data were analyzed using an automated bioinformatics pipeline designed to detect various genetic alterations, including single-nucleotide variations, insertions and deletions, gene amplifications and deletions, and gene fusions.

Quantitative Polymerase Chain Reaction (qPCR)

Genomic DNA was isolated from Formalin-Fixed Paraffin-Embedded (FFPE) tumor specimens, and *IRS2* and *MYCL* copy number amplification was performed by the PRISM 7900HT Fast Real-Time PCR System (Applied Biosystems). All qPCR reactions were performed in triplicate using the SYBR Green method. The PCR conditions were: preheating at 50°C for 2 min; 95°C for 10 min; 40 cycles at 95°C for 15 s, and 60°C for 1 min. *IRS2* copy numbers were calculated from a standard curve constructed from normal DNA amplification in comparison to *ALB*, located at 4q11-q13, and normalized to the normal tissue genomic DNA. Finally, the number of amplification for *IRS2* was calculated as follows: copy number of the target gene (*IRS2*)/copy number of the reference gene (*ALB*). Primers for *IRS2* and *MYCL* copy number analysis were the following: IRS2 forward, 5′-F CTTTAGTTGGCTGGCTCTGG-3′; *IRS2* reverse, 5′-GTTGTC TGCTCCTGCGAATAG-3′; MYCL forward, 5′-GGGTCTGCCT TTT GTTCTTATCT-3′; *MYCL* reverse, 5′-AAAGGAGGGGACAT TAGCAAG-3′; *ALB* forward, 5′-TGAAACATACGTTCCCAAAG AGTTT-3′; ALB reverse, 5′-CTCTCCTTCTCAGAAA GTGTGCA TAT-3′. PCR products were purified using a PCR purification kit and directly sequenced by standard procedures using forward and reverse primers.

Microarray Experiments

Two patients (designated as 033 T and 694 T and PDXs 033 T and 694 T) were investigated, and a complete case set comprised a primary tumor sample and corresponding xenografts. Total RNA was extracted from the patient tissues and xenografts containing >80% tumor cell content. Extracted RNA was hybridized to Agilent 60 K expression microarrays, according to the manufacturer's instructions.

In Vitro Drug Sensitivity Assay

Primary cultures of PDX cells in the serum-free sphere culture conditions were seeded in 384-well plates, at 500 cells per well. Two hours after plating, the cells were treated with a drug library in 3-fold and 10-point serial dilutions (n = 3, for each condition). Cells were incubated for 6 days at 37°C, in a 5% CO_2 humidified incubator, and the cell viability was analyzed using an adenosine triphosphate monitoring system based on firefly luciferase (ATPlite 1step; PerkinElmer, Waltham, MA, USA). The drug library comprised 43 targeted agents that were included in the clinical guidelines or the present clinical trials for the treatment of lung cancer (Table S1). All drugs were purchased from Selleckchem (Houston, TX, USA). The drugs were stored and diluted according to the manufacturer's instructions. The tested concentrations for each drug were empirically derived in order to investigate a clinically relevant spectrum of drug activities. IC_{50} values were calculated as an average of triplicate experiments using S+ Chip Analyzer (Samsung Electro-Mechanics, Suwon, Korea). In order to investigate the effects of the treatment with targeted agents, signal transduction assays were performed.

Western Blotting

IRS2 high-expressing cells were transfected with short hairpin RNA (shRNA) against control sequence, and IRS2 low-expressing cells were transiently transfected with IRS2 for 48–72 h, followed by treatment with or without ceritinib for 48–72 h at different concentrations. Cells were then harvested for whole cell lysates with RIPA buffer (50 mM HEPES [pH 7.5], 0.1% SDS, 1% NP-40, 0.5% sodium deoxycholate, 150 mM NaCl, 50 mM NaF, 1 mM Na_2VO_4, 1 mM nitrophenylphosphate, and protease inhibitors). Immunoblotting was performed with the following antibodies: phospho-AKT (Ser473; Cell Signaling Technology, 9271), AKT (Cell Signaling Technology, 9272), GAPDH (Santa Cruz Biotechnology, sc-25,778), β-actin (Santa Cruz Biotechnology, sc-47778), and IRS2 (Cell Signaling Technology, 3089S).

Xenograft Mouse Models

Nude mice (Orient Bio, Sungnam, Korea) were used for *in vivo* studies and were cared for in accordance with the guidelines approved by the Samsung Biomedical Research Institute (protocol No. H-A9–003) and the Institute of Laboratory Animal Resources Guide. 8-week-old female mice were injected subcutaneously with 5 million A375P cells together with Matrigel. Once tumors reached an average volume of 100 mm^3, mice were randomized to the different treatment cohorts; that is, they were randomized to receive ceritinib (20 or 50 mg/kg body weight per os (p.o.) daily for 17 days) or vehicle control (n = 5 for LDK-378, 20 mg or 50 mg; n = 5 for vehicle control). Mice were observed daily throughout the treatment period for signs of morbidity and/or mortality. Tumors were measured twice weekly using calipers, and tumor volume was calculated using the formula: length × $width^2$ × 0.52. Body weight was also assessed twice weekly. The p values were determined with the Wilcoxon rank-sum test.

Statistical Analysis

The Mann-Whitney U and chi-square tests were used to evaluate the differences between groups in both *in vitro* and *in vivo* assays. All statistical experiments were two sided, and p values < 0.05 were considered as statistically significant. SPSS software (v.17.0; Chicago, IL, USA) was used for all statistical analyses.

SUPPLEMENTAL INFORMATION

Supplemental Information can be found online at https://doi.org/10.1016/j.omto.2019.12.009.

AUTHOR CONTRIBUTIONS

M.-S.L., K.J., D.-Y.O., and Y.-L.C. designed the experiments and wrote the manuscript. M.-S.L., K.J., and J.-Y.S. conducted all the experiments. M.-J.S., S.-B.A., and B.L. contributed to specimen

collection and sample preparation. D.-Y.O. and Y.-L.C. supervised the project. All authors discussed the results and contributed to the final manuscript.

CONFLICTS OF INTEREST

The authors declare no competing interests.

ACKNOWLEDGMENTS

This work was supported by National Research Foundation of Korea (NRF) grants funded by the Korean government (Ministry of Science, ICT, and Future Planning) (nos. 2016R1A5A2945889, 2019R1A2B5B02069979, and 2018R1C1B6001396).

REFERENCES

1. Koinis, F., Kotsakis, A., and Georgoulias, V. (2016). Small cell lung cancer (SCLC): no treatment advances in recent years. Transl. Lung Cancer Res. *5*, 39–50.
2. Gazdar, A.F., Bunn, P.A., and Minna, J.D. (2017). Small-cell lung cancer: what we know, what we need to know and the path forward. Nat. Rev. Cancer *17*, 725–737.
3. Bunn, P.A., Jr., Minna, J.D., Augustyn, A., Gazdar, A.F., Ouadah, Y., Krasnow, M.A., Berns, A., Brambilla, E., Rekhtman, N., Massion, P.P., et al. (2016). Small cell lung cancer: can recent advances in biology and molecular biology be translated into improved outcomes? J. Thorac. Oncol. *11*, 453–474.
4. Kim, D.W., Kim, H.G., Kim, J.H., Park, K., Kim, H.K., Jang, J.S., Kim, B.S., Kang, J.H., Lee, K.H., Kim, S.W., et al. (2019). Randomized phase III trial of irinotecan plus cisplatin versus etoposide plus cisplatin in chemotherapy-naïve Korean patients with extensive-disease small cell lung cancer. Cancer Res. Treat. *51*, 119–127.
5. Abidin, A.Z., Garassino, M.C., Califano, R., Harle, A., and Blackhall, F. (2010). Targeted therapies in small cell lung cancer: a review. Ther. Adv. Med. Oncol. *2*, 25–37.
6. George, J., Lim, J.S., Jang, S.J., Cun, Y., Ozretić, L., Kong, G., Leenders, F., Lu, X., Fernández-Cuesta, L., Bosco, G., et al. (2015). Comprehensive genomic profiles of small cell lung cancer. Nature *524*, 47–53.
7. Mori, N., Yokota, J., Akiyama, T., Sameshima, Y., Okamoto, A., Mizoguchi, H., Toyoshima, K., Sugimura, T., and Terada, M. (1990). Variable mutations of the RB gene in small-cell lung carcinoma. Oncogene *5*, 1713–1717.
8. Takahashi, T., Takahashi, T., Suzuki, H., Hida, T., Sekido, Y., Ariyoshi, Y., and Ueda, R. (1991). The p53 gene is very frequently mutated in small-cell lung cancer with a distinct nucleotide substitution pattern. Oncogene *6*, 1775–1778.
9. Wistuba, I.I., Gazdar, A.F., and Minna, J.D. (2001). Molecular genetics of small cell lung carcinoma. Semin. Oncol. *28* (2, Suppl 4), 3–13.
10. Dziadziuszko, R., Camidge, D.R., and Hirsch, F.R. (2008). The insulin-like growth factor pathway in lung cancer. J. Thorac. Oncol. *3*, 815–818.
11. Tao, Y., Pinzi, V., Bourhis, J., and Deutsch, E. (2007). Mechanisms of disease: signaling of the insulin-like growth factor 1 receptor pathway–therapeutic perspectives in cancer. Nat. Clin. Pract. Oncol. *4*, 591–602.
12. Qu, X., Wu, Z., Dong, W., Zhang, T., Wang, L., Pang, Z., Ma, W., and Du, J. (2017). Update of IGF-1 receptor inhibitor (ganitumab, dalotuzumab, cixutumumab, teprotumumab and figitumumab) effects on cancer therapy. Oncotarget *8*, 29501–29518.
13. Park, E., Park, S.Y., Kim, H., Sun, P.L., Jin, Y., Cho, S.K., Kim, K., Lee, C.T., and Chung, J.H. (2015). Membranous insulin-like growth factor-1 receptor (IGF1R) expression is predictive of poor prognosis in patients with epidermal growth factor receptor (EGFR)-mutant lung adenocarcinoma. J. Pathol. Transl. Med. *49*, 382–388.
14. Xu, H., Lee, M.S., Tsai, P.Y., Adler, A.S., Curry, N.L., Challa, S., Freinkman, E., Hitchcock, D.S., Copps, K.D., White, M.F., et al. (2018). Ablation of insulin receptor substrates 1 and 2 suppresses *Kras*-driven lung tumorigenesis. Proc. Natl. Acad. Sci. USA *115*, 4228–4233.
15. Reuveni, H., Flashner-Abramson, E., Steiner, L., Makedonski, K., Song, R., Shir, A., Herlyn, M., Bar-Eli, M., and Levitzki, A. (2013). Therapeutic destruction of insulin receptor substrates for cancer treatment. Cancer Res. *73*, 4383–4394.
16. Huang, F., Chang, H., Greer, A., Hillerman, S., Reeves, K.A., Hurlburt, W., Cogswell, J., Patel, D., Qi, Z., Fairchild, C., et al. (2015). IRS2 copy number gain, KRAS and BRAF mutation status as predictive biomarkers for response to the IGF-1R/IR inhibitor BMS-754807 in colorectal cancer cell lines. Mol. Cancer Ther. *14*, 620–630.
17. Iwakawa, R., Takenaka, M., Kohno, T., Shimada, Y., Totoki, Y., Shibata, T., Tsuta, K., Nishikawa, R., Noguchi, M., Sato-Otsubo, A., et al. (2013). Genome-wide identification of genes with amplification and/or fusion in small cell lung cancer. Genes Chromosomes Cancer *52*, 802–816.
18. Day, E., Poulogiannis, G., McCaughan, F., Mulholland, S., Arends, M.J., Ibrahim, A.E., and Dear, P.H. (2013). IRS2 is a candidate driver oncogene on 13q34 in colorectal cancer. Int. J. Exp. Pathol. *94*, 203–211.
19. Oh, D.Y., Jung, K., Song, J.Y., Kim, S., Shin, S., Kwon, Y.J., Oh, E., Park, W.Y., Song, S.Y., and Choi, Y.L. (2017). Precision medicine approaches to lung adenocarcinoma with concomitant MET and HER2 amplification. BMC Cancer *17*, 535.
20. Rudin, C.M., and Poirier, J.T. (2017). Small-cell lung cancer in 2016: shining light on novel targets and therapies. Nat. Rev. Clin. Oncol. *14*, 75–76.
21. Semenova, E.A., Kwon, M.C., Monkhorst, K., Song, J.Y., Bhaskaran, R., Krijgsman, O., Kuilman, T., Peters, D., Buikhuisen, W.A., Smit, E.F., et al. (2016). Transcription factor NFIB is a driver of small cell lung cancer progression in mice and marks metastatic disease in patients. Cell Rep. *16*, 631–643.
22. Wu, N., Jia, D., Ibrahim, A.H., Bachurski, C.J., Gronostajski, R.M., and MacPherson, D. (2016). NFIB overexpression cooperates with Rb/p53 deletion to promote small cell lung cancer. Oncotarget *7*, 57514–57524.
23. You, H.L., Liu, T.T., Weng, S.W., Chen, C.H., Wei, Y.C., Eng, H.L., and Huang, W.T. (2018). Association of IRS2 overexpression with disease progression in intrahepatic cholangiocarcinoma. Oncol. Lett. *16*, 5505–5511.
24. Kubota, N., Kubota, T., Itoh, S., Kumagai, H., Kozono, H., Takamoto, I., Mineyama, T., Ogata, H., Tokuyama, K., Ohsugi, M., et al. (2008). Dynamic functional relay between insulin receptor substrate 1 and 2 in hepatic insulin signaling during fasting and feeding. Cell Metab. *8*, 49–64.
25. Porter, H.A., Perry, A., Kingsley, C., Tran, N.L., and Keegan, A.D. (2013). IRS1 is highly expressed in localized breast tumors and regulates the sensitivity of breast cancer cells to chemotherapy, while IRS2 is highly expressed in invasive breast tumors. Cancer Lett. *338*, 239–248.
26. Mercado-Matos, J., Janusis, J., Zhu, S., Chen, S.S., and Shaw, L.M. (2018). Identification of a novel invasion-promoting region in insulin receptor substrate 2. Mol. Cell. Biol. *38*, e00590-17.
27. Friboulet, L., Li, N., Katayama, R., Lee, C.C., Gainor, J.F., Crystal, A.S., Michellys, P.Y., Awad, M.M., Yanagitani, N., Kim, S., et al. (2014). The ALK inhibitor ceritinib overcomes crizotinib resistance in non-small cell lung cancer. Cancer Discov. *4*, 662–673.
28. Beasley, M.B., Brambilla, E., and Travis, W.D. (2005). The 2004 World Health Organization classification of lung tumors. Semin. Roentgenol. *40*, 90–97.
29. Groome, P.A., Bolejack, V., Crowley, J.J., Kennedy, C., Krasnik, M., Sobin, L.H., Goldstraw, P., et al.; IASLC International Staging Committee; Cancer Research and Biostatistics; Observers to the Committee (2007). The IASLC Lung Cancer Staging Project: validation of the proposals for revision of the T, N, and M descriptors and consequent stage groupings in the forthcoming (seventh) edition of the TNM classification of malignant tumours. J. Thorac. Oncol. *2*, 694–705.